

Cellular automata modeling of propagation and absorption of acoustic waves in impedance tube

Meng WANG¹; Bo ZHANG^{1,2} Qiqi CHEN¹; Liheng WANG¹; Yutian BAI¹

¹ School of Mechanical Engineering, Ningxia University, China

² CAE Key Laboratory for Intelligent Equipment of Ningxia, China

ABSTRACT

A one-dimensional Cellular Automata (CA) model for acoustic wave's propagation and absorption in impedance tube with and without porous metals is studied to explore acoustic absorbing properties of porous metal in multiple physical fields. In cellular space, wave motion equation for small amplitude travelling waves at room temperatures and normal sound pressure levels is reconstructed by using finite differential method; accordingly, local evolutionary rules of each cell are deduced out. Provided that a specific sound source is definitely given, the sound pressure distribution inside impedance tube can be obtained by solving this CA model. Based on above CA theory and classical acoustic models of porous materials, the evolutionary rules of cell for the case that porous material is placed at the end of impedance tube are formulated. And sound absorption coefficient of porous materials may be calculated as well. Finally, the effects of temperature and sound pressure level on nonlinear propagation properties of acoustic travelling waves with finite amplitude are analysed by rewriting Westervelt wave motion equation in the form of finite differential. In this way, one may predict sound absorption of porous material at different temperatures and sound pressure levels. The results from CA model agree well with experimental data.

Keywords: Cellular Automata, Sound Pressure Distribution, MATLAB

1. INTRODUCTION

Porous metal materials are widely used in extreme environments such as high temperature, high pressure, and strong air flow. The interior of the material is composed of metal skeleton and many voids, which can effectively absorb sound energy and reduce noise. Porous metal materials have a series of excellent properties such as high specific strength, high specific stiffness and good corrosion resistance. Therefore, porous metal materials can be used as a sound absorbing material in aircraft engine cabin (1). Noise is essentially a mechanical wave, and as it propagates in high temperature or imperfect media, energy transformation may occur to attenuate the sound waves and achieve sound absorption. However, when we study the problem of sound transmission in extreme environment, we often need to solve high-order differential equation. At the same time, the three theoretical models for studying the internal structure and sound absorption properties of porous materials also involve many factors affecting the structural complexity of material, which all make the research difficult. Jihui Wu et al. used transfer-function method to measure the sound absorption coefficient of materials at different temperatures (2). Bo Zhang et al. used wave equation method to study the sound absorption properties of porous metal materials at high temperatures (3). However, their results are not in good agreement with the experimental results.

Cellular Automata (CA) as a numerical algorithm is very suitable for the simulation of a complicated physical system. It is based on the principle of local action. It is a process of advancing and adjusting repeatedly to reach the system balance (4).

2. ACOUSTIC MODELING OF CELLULAR AUTOMATA

We take the impedance tube as the research object, and place the impedance tube in two dimensions, and divide it into cells according to the time step and space step. There are four different types of cells.

¹ zhangb@nxu.edu.cn

² 12712580@qq.com

The cells in the first column belong to sound source cells, and the source excitation is a given plane wave; note that the state variables of the source remain constant. The neighboring cell is the air medium cell, which is next to the sound source. Cell state will be affected by the sound source at the initial time, the sound absorbing medium cell of porous metal material is followed by air medium cell. The number of the cell is determined according to the material thickness. The cells in the last column stand for rigid media. There are different local transfer rules between cells at different locations. The state variables of each cell in different time steps can be obtained by MATLAB programming.

2.1 Rules in Air Media

We assume that the waves in impedance tube do not contain non-planar wave components, and all sound waves are planar waves. Therefore, there is no reflection at the upper and lower boundaries of each column.

The space step is 1 mm and the impedance tube length is set to be 1m, so there are 1002 cells in total in the model. The first and 1002th cells stand for sound source and rigid wall, respectively, and the second to 1001 cells are sound medium parts. We define that each cell has two state variables: excess sound pressure (i.e. sound pressure) and change of sound pressure. At normal pressure and temperature, we use the one-dimensional wave equation of small amplitude sound wave.

$$\frac{\partial^2 p}{\partial x^2} = \frac{1}{c_0^2} \frac{\partial^2 p}{\partial t^2} \quad (1)$$

By algebraic transformation, as follows,

$$\frac{p(x+dx,t) - 2p(x,t) + p(x-dx,t)}{dx^2} = \frac{1}{c_0^2} \frac{p(x,t+dt) - 2p(x,t) + p(x,t-dt)}{dt^2} \quad (2)$$

the local evolutionary rules of sound wave propagation in air medium can be obtained:

$$p(ix, jt+1) = \frac{dt^2(p(ix+1, jt) - 2p(ix, jt) + p(ix-1, jt))}{dx^2} - p(ix, jt-1) + 2p(ix, jt) \quad (3)$$

The first cell on the left is the sound source cell, so the plane wave is :

$$p = P_0 e^{j(\omega t + \frac{\pi}{2})} \quad (4)$$

Starting from step 1002, standing wave arises due to the superposition of incident and reflected sound pressures in tube, which is expressed as:

$$p = 2p \cdot \cos(kx) e^{j\omega t} \quad (5)$$

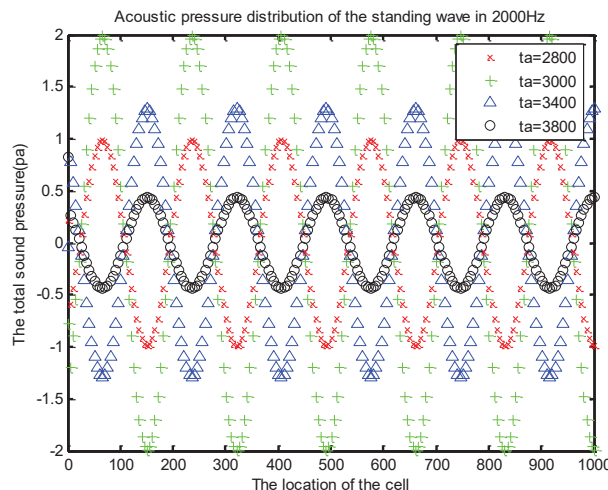


Figure 1 – Sound Pressure Distribution

It can be seen from the figure that the position of the standing wave crest and trough does not change with time, and the maximum value of the amplitude is 2Pa and the minimum value is -2Pa. The result is reasonable.

We further add some porous sound-absorbing materials, and the flow resistance of the materials can be determined by the definition below,

$$\sigma_0 = \frac{\Delta p}{v\phi d} \quad (6)$$

Here, Δp corresponds to the variation of sound pressure, and then deduces as follow:

$$\sigma_0 = \frac{p(ix, jt) - p(ix, ji-1)}{v\phi d} \quad (7)$$

The local rules of the impedance tube having sound absorbing medium can be obtained also:

$$p(x, t+1) = p(x, t) + \Delta p(x, t+1) \left[\frac{1 - \frac{\sigma\phi}{Z_c}}{1 + \frac{\sigma\phi}{Z_c}} \right] \quad (8)$$

It can be seen from the formula that the sound pressure at this moment is related to the properties of the material itself and the sound pressure at the cell at the previous moment. Furthermore, we need to calculate the characteristic impedance of metal materials. There are three sound absorption models: empirical model (D-B model), phenomenological model (J-C-A model) and flow around model. In this work, we use phenomenological models to calculate sound absorbing of porous metal.

2.2 CA Simulation Based on J-C-A Phenomenological Model

J-C-A model needs not only two parameters of porosity and flow resistance, but also other five parameters such as tortuosity factor, thermal characteristic length and viscous characteristic length. The bulk modulus K_{eff} and effective density ρ_{eff} are given in the model (5):

$$K_{eff} = \gamma P_0 \left[\gamma - (\gamma - 1) \left(1 + \frac{8\eta}{i\omega L_{th}^2 B^2 \rho_0} \sqrt{1 + \frac{i\omega L_{th}^2 B^2 \rho_0}{16\eta}} \right)^{-1} \right]^{-1} \quad (9)$$

$$\rho_{eff} = \tau \rho_0 \left[1 + \frac{\sigma_0 \phi}{i\omega \rho_0 \tau} \sqrt{1 + \frac{4i\omega \tau^2 \eta \rho_0}{\sigma_0^2 L_v^2 \phi^2}} \right] \quad (10)$$

In Eqn. (9) and Eqn. (10), ρ_0 is the static density of air, η is the viscosity coefficient of air, γ is the specific heats of air, B is the Prandtl constant, ϕ is porosity, σ_0 is flow resistivity, L_v is viscous characteristic constant, L_{th} is thermal characteristic constant. Characteristic impedance of material is:

$$Z_c = \sqrt{K_{eff} \cdot \rho_{eff}} \quad (11)$$

It is noticed that in this paper, the sound absorption coefficient of materials is evaluated by using standing wave method:

$$\alpha = 1 - \left(\frac{\frac{|P|_{max} - 1}{|P|_{min}}}{\frac{|P|_{max} + 1}{|P|_{min}}} \right)^2 \quad (12)$$

In the formula, we need to get the maximum and minimum of sound pressure. Since we have obtained the distribution of the sound pressure, we can easily extract the maximum and minimum of that to get the sound absorption coefficient.

3. MODEL OPTIMIZATION AT HIGH TEMPERATURE

In a complicated high environment, in theory, the internal structure of porous materials may be modified accordingly, thus some structural or acoustic parameters more or less change with the increase of temperature. Considering non-uniform high temperature fields, one way use the following wave equation in this subsection (2).

$$\frac{d^2 p}{dz^2} + 2\alpha(\lambda, \lambda_t) \frac{dp}{dz} + k_0(\lambda, \lambda_t)^2 p = 0 \quad (13)$$

And two functions in Eqn. (13) are as follows:

$$k_0(\lambda, \lambda_t)^2 = \alpha_\infty \frac{\omega^2}{c_0^2} \frac{1}{F(\lambda)} (\gamma - (\gamma - 1)F(\lambda_t)) \quad (14)$$

$$\alpha(\lambda, \lambda_t) = 0.5 \frac{1}{F(\lambda)} \left[\frac{dF(\lambda)}{d\lambda} \frac{d\lambda}{dT_0} + \frac{1}{T_0} \left[\frac{\alpha_\infty (F(\lambda_t) - B^2 F(\lambda))}{1 - B^2} \right] \right] \frac{1}{\alpha_\infty^{0.5}} \frac{dT_0}{dz} \quad (15)$$

In Eqn. (15), dT_0/dz is temperature gradient and if the temperature is constant, its value is equal to zero. Local rules with temperature gradient and without temperature gradient can be gained by differential treatment of the equation.

$$p(z+1) = (2 - dz^2 k_0(\lambda, \lambda_t)^2) p(z) - p(z-1) \quad (16)$$

$$p(z+1) = (2 - 2\alpha(\lambda, \lambda_t) dz - dz^2 k_0(\lambda, \lambda_t)^2) p(z) + (2\alpha(\lambda, \lambda_t) dz - 1) p(z-1) \quad (17)$$

The relationship between acoustic constants and temperature is as follows:

$$\frac{\rho_0}{\rho_1} = \frac{T_1}{T_0} \quad (18)$$

$$\sigma(T) = \sigma(T_c) (T/T_c)^{3/2} (T_c + T_s)/(T + T_s) \quad (19)$$

$$B^2 = 0.5658T^{0.04} \quad (20)$$

Among them, ρ_0 is the air density at room temperature, ρ_1 is the air density at high temperature, T_0 is the absolute temperature at room temperature, T_1 is the absolute temperature at high temperature. In Eqn. (18), $T_c=300$ K, and $T_s=110.4$ K.

4. MODEL OPTIMIZATION UNDER HIGH SOUND PRESSURE

When the sound pressure rises to a certain value, particle velocity is no longer a negligible quantity compared to the sound velocity, so the problem at this time belongs to nonlinear acoustics.

In non-linear acoustics, the trace in the equation will be retained to the second order trace and Westervelt equation is considered as:

$$\nabla^2 p - \frac{1}{c_0^2} \frac{\partial^2 p}{\partial t^2} - \frac{\delta}{c_0} \frac{\partial^3 p}{\partial t^3} + \frac{\beta}{\rho_0 c_0^4} \frac{\partial^2 p^2}{\partial t^2} = 0 \quad (21)$$

After rewriting each term of the equation above by using the difference method, the cell sound pressure value at a certain position at time $t+1$ can be obtained:

$$p(t+1) = \frac{1}{P1} \left[c_0^2 \frac{(dt)^2}{(dx)^2} p(t, x+1) - 2p(t, x) + p(t, x-1) + P2 p(t, x) - P3 p(t-1, x) \right] + \frac{P4}{P} [34p(t-2, x) - 24p(t-3, x) + 8p(t-4, x) - p(t-5, x)] \quad (22)$$

$$P1 = 1 - \frac{4\beta}{\rho_0 c_0^2} p(t, x) + \frac{2\beta}{\rho_0 c_0^2} p(t-1, x) \quad (23)$$

$$P2 = 2 + \frac{3\delta}{c_0^2 dt} - \frac{6\beta}{\rho_0 c_0^2} p(t, x) + \frac{4\beta}{\rho_0 c_0^2} p(t-1, x) \quad (24)$$

$$P3 = 1 + \frac{23\delta}{2c_0^2 dt} \quad (25)$$

$$P4 = \frac{\delta}{2c_0^2 dt} \quad (26)$$

With the increase of sound pressure, not only the wave equation of sound wave transmission changes, but the sound absorption property of materials does, the most obvious of which is the change of material flow resistance. In the case of finite amplitude, the flow resistance rate no longer obeys Darcy's linear law. We adopt Hongyuan Jiang's formula (6) for calculating flow resistance.

$$\sigma = \sigma_0 + \frac{1.42(1-\phi)}{2\phi^3 da} \rho_0 |u| \quad (27)$$

In Eqn. (26), σ_0 , ϕ , da , ρ_0 , u are static flow resistivity, porosity, pore size, equivalent density, and particle velocity. Starting from the one-dimensional non-linear motion equation, one may get the one-dimensional non-linear continuity equation of porous materials at high sound pressure levels in the following form:

$$\frac{\partial^2 v}{\partial x^2} = \omega^2 \frac{\rho_{eff}}{K} v - j\omega \frac{8\mu_0}{3\pi K} v|v| \quad (28)$$

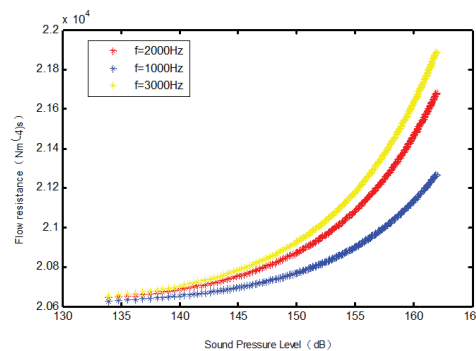


Figure 2 – Sound Pressure Distribution

The Fig. 2 shows the distribution of material flow resistance with respect to incident sound pressure level at frequencies of 1000Hz, 2000Hz and 3000Hz. It can be seen that the material flow resistance increases nonlinearly with the increase of sound pressure level.

5. SIMULATION RESULTS AND ANALYSIS

Based on the theory in previous sections, we employ J-C-A model to conduct a more comprehensive simulation analysis of the system. Considering the changes of some parameters of materials relative to those at room temperature, the sound absorption coefficient of the system is simulated at high temperature and high sound pressure.

Table (1) gives the physical and acoustical parameters of samples under consideration. The Cellular Automaton model based on J-C-A model is used to simulate the sound absorption coefficient of the material at room temperature; the result is shown in Fig. 3.

Table 1 – Physical and acoustical parameters of samples

Materials	Porosity	Flow resistance, N.s/m ⁴	Thickness, mm	Tortuosity factor	Thermal length, μm	Viscous length, μm
Sample 1	90.89	20610	25	1.664	123.19	289.54
Sample 2	90	2100	30	1.305	206.10	210.20
Sample 3	80	3095	30	1.170	116.66	313.34
Sample 4	90	1993	20	1.380	210.73	215.36
Sample 5	80	2140	30	1.324	242.85	325.96

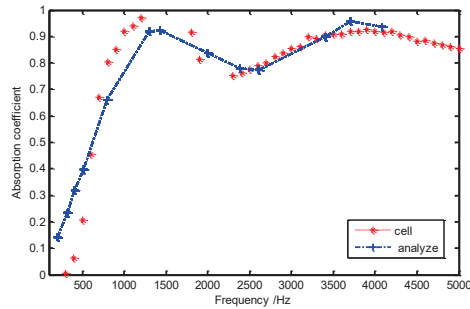
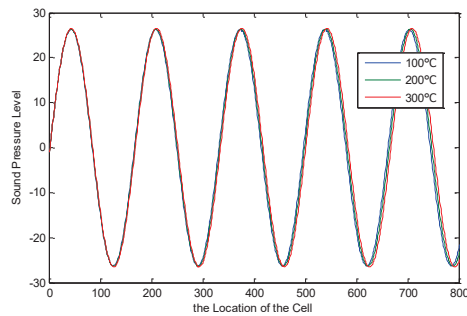
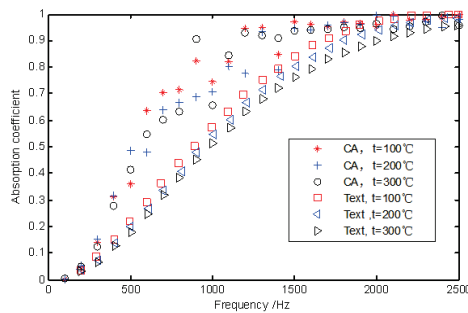


Figure 3 –Sound Absorption Coefficient Curves

Figure 4 shows the sound pressure level distribution and sound absorption coefficient curves of porous sample 1 at 100,200,300 degrees Celsius, respectively, in literature (2).



(a) Sound Pressure Level Distribution



(b) Sound Absorption Coefficient Curves at high temperatures

Figure 4 –Simulation Result at Different Temperatures

It can be seen that the sound absorption performance of the material decreases with the increase of temperature, because the flow resistance of the material increases further with the increase of temperature. And, it can be seen that the error from cellular automata model is quite large, the possible reason of which is from the choice of step size in simulations and the error of experiment itself.

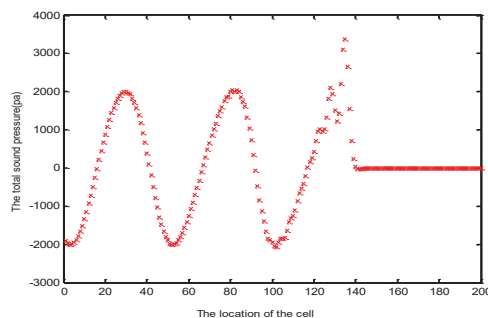


Figure 5 – Sound Pressure Distribution

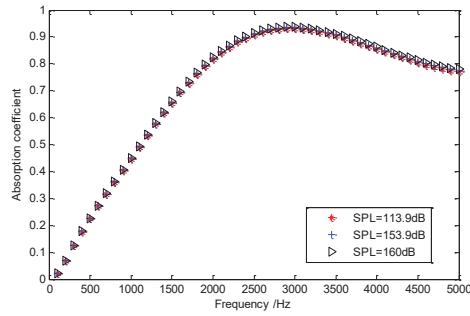


Figure 6 – Sound Absorption Coefficient Distribution

Figure 5 shows the sound pressure distribution in impedance tube, roughly a standing wave with an amplitude of 2000 Pa and a frequency of 1500Hz. Because of the nonlinear distortion, the waveform inside impedance tube is no longer a theoretical sinusoidal wave, but more than a shock wave finally. Fig. 6 shows the distribution of sound absorption coefficients of sample# 1 with amplitudes of sound source up to 1000Pa, 2000Pa, and 3000Pa, respectively.

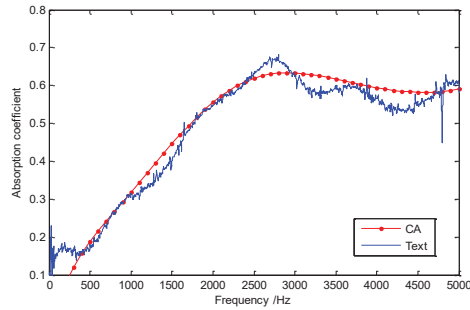


Figure 7 – Sound Absorption Coefficient Curves of Sample 2

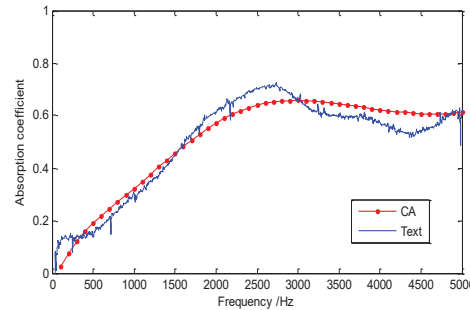


Figure 8 – Sound Absorption Coefficient Curves of Sample 3

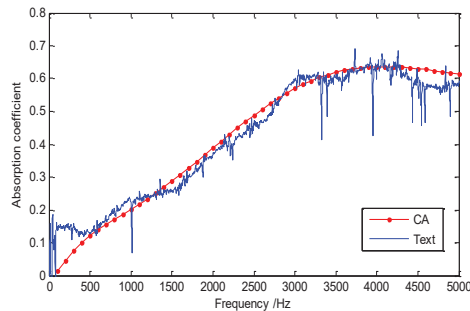


Figure 9 – Sound Absorption Coefficient Curves of Sample 4

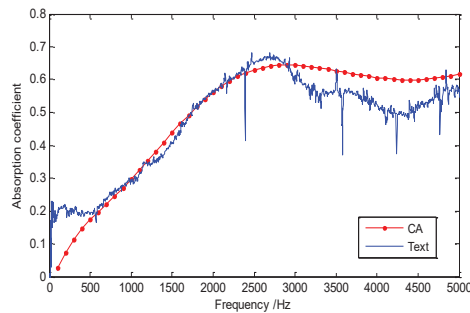


Figure 10 – Sound Absorption Coefficient Curves of Sample 5

Figures 7 to 10 show that by introducing the parameters in Table 1 into the presented Cellular Automata model, the sound absorption coefficients of materials at 125dB can be obtained. It can be found out that as a whole, the simulated and experimental results fit quite well, but there still exists relatively large errors at some frequencies.

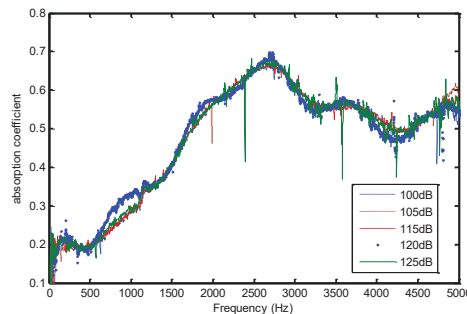


Figure 11 – Sound Absorption Coefficient Curves of Sample 5 at Different Sound Pressure Levels

6. CONCLUSIONS

In this work, the acoustic model of one-dimensional Cellular Automata is built up by modifying linear acoustic wave equation for different environment conditions. It can be seen that, normally, as the temperature increases, the viscosity and the density of air change accordingly, which makes the sound absorption coefficient of material decrease at high temperature. According to the experimental and simulation results, the change of sound absorption coefficient is not obvious as the sound pressure level increases. To our knowledge, the tendency above may be due to that the strength of sound source in simulation or experiment is not large enough to apparently affect sound absorption of materials.

ACKNOWLEDGEMENTS

The authors gratefully acknowledge supports for this work from the Graduate Innovative Educational Project of Ningxia (Grant No. YKC201606), Research Project of CAE Key Laboratory for Intelligent Equipment of Ningxia, Project of National Natural Science Foundation of China (Grant No. 51365046), and Graduate Innovative Project of Ningxia University (Grant No. GIP2018055).

REFERENCES

1. Han Z, Jiuhu W, Zhiping Zhou, H. Sound absorbing property of porous metal materials with high temperature and high sound pressure by turbulence analogy. *Journal of Applied Physics*. 2013;113(19):336-337.
2. Bo Z, Tianning C, Kai F, Hualin C. High temperature absorption performance of sintered metal fiber porous materials. *Journal of Xi'an Jiaotong University*. 2008;42(11):1327-1331.
3. Fugui S, Hualin C, Jiuhu W. Performance test and research on high temperature absorption of porous metal materials. *Journal of Vibration Engineering*. 2010;23(05):502-507.
4. Xinji Y. The parallel cellular element method. *Computational Mechanics*. 2006;23(1):35-37.
5. Allard JF. *Propagation of sound in porous media*. Elsevier Applied Science, London: 1993, p. 92-100.
6. Hongyuan J, Guoqi W. Nonlinear Sound absorption performance of metal rubber. *Journal of Mechanical Engineering*. 2010;49(19):70-77.